A CIT Reconstruction Algorithm Using Volumetric Constraints

Chaitali Biswas and Helen R. Na
Department of Electrical Engineering,
University of California, Los Angeles, CA 90095–1594, USA.

1996

Abstract *CIT image reconstruction using information regarding shape of the electron density distribution in the plane of interested is implemented using a volumetric iterative techinique. Shape estimation and guidance is provided on a localized basis both in the projection and image domains of the algebraic reconstruction process. Preliminary results of IRI-90 based simulations indicate substantial improvement in vertical resolution even for a priori sets which are very different from the test image.*

Introduction

The set of ionospheric TEC data obtained from a standard CIT imaging system is not sufficient for describing the electron density distribution pattern in the two-dimensional ionospheric plane of interest. As shown in Figure 1, this image plane lies in between the satellite orbit and the chain of ground station receivers. The differential Doppler shift between the dual frequency satellite signals received at the ground stations correspond to the cumulative electron densities encountered by the corresponding ray path. Preliminary processing of the signals including correction for station offsets yields values of total electron content of the ionosphere along the ray paths. Assuming that ray paths pass without significant distortion or diffraction through the atmosphere, it is possible to map the coverage of the the plane of interest by the satellite positions and ground station locations. For the purpose of this study, all ground stations were assumed to be coplanar with the satellite orbit and evenly spaced along the chain. Figure 1 shows how the curvature of the earth, continuity of the ionospheric shell around it and restrictions on minimum ray elevation at ground stations, prevent recording of TEC information along near horizontal ray paths.

Therefore, when TEC readings from various receivers are regrouped according to angle of ray incidence to form pseudo tomographic projections, the sets with near horizontal rays lack in measured TEC information.

This information deficiency is manifested in the reconstructed image as a lack of variation in the vertical or altitudinal direction. For example, it is difficult to identify heights of maximum and minimum electron densities such as peaks, troughs and saddle points on the ionospheric image. A popular means of providing reliable vertical information in the reconstruction process is to add information from ionospheric models or known facts from ionospheric physics. Some TEC inversion algorithms rely on a priori information about vertical distribution, either introducing it as an initial guess into an iterative algebraic reconstruction process while some others, impose smoothness constraints and extremal nullity to ensure that electron density is maximized within an acceptable altitude range, usually between 100 and 500 km altitude.

Projection Domain Volumetric Correction

This paper introduces the concept of balanced a priori selection and incorporation during an other-

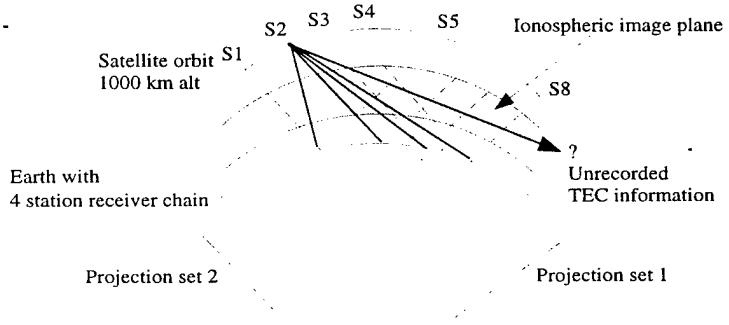

Figure 1. CIT imaging system geometry

wise standard SIRT Simultaneous Iterative Algebraic Reconstruction Technique (SIRT) process.

Consider the flowchart for standard SIRT reconstruction presented in Figure 2. In each iteration the difference between the TEC calculated for a ray from the current reconstruction and the measured TEC is stored as an element of the error vector. After the error vector has been completely updated, each error value is redistributed along the ray path as defined by the system matrix A. During the redistribution the quantity of error-based correction received by any individual pixel along the ray depends only on the length of the ray lying within it. Hence, no altitude dependent distribution is achieved in the correction process. The cumulative correction for each pixel obtained from all relevant projections is then subtracted from the current distribution to obtain the image for the next iteration. The reconstruction process is usually terminated either after the correction image values satisfy some stipulated bounds or the number of iterations exceeds a maximum.

Figure 3 shows the inclusion of shape information during the projection domain redistribution of error values along various ray paths. Insufficiency of information regarding electron density profiles along any ray path can be partially compensated for by computing a desirable distribution pattern along it. In the Volumetric SIRT (VSIRT) algorithm, this profile was computed from a set of a priori profiles based on the difference in TEC values from the current reconstruction and a priori images. The optimal profile was defined as the weighted sum of normalized profiles from various a priori images. The weights are calculated as the inverse Euclidean distances in TEC value space, followed by normalization. In case the errors of one or more a priori TECs come significantly close to the calculated value, those a priori image profiles are exclusively selected for the distribution process thus providing options for selection rather than enforcing the principle of combination at all times.

Image Domain Volumetric Correction

Once TEC based error corrections have been made to the image, it is necessary to provide some means of balancing the information update within user defined local neighborhoods in the image domain. As shown in Figure 4, a shape matrix S (X-m-1)x(Y-n-1) for an XxY image is hereby defined as the truncated convolution of the image with a (2m+1)x(2n+1) mask, shifted and normalized to lie in the closed interval [0,1]. If the mask is chosen to be a normalized two-dimensional low pass filter such as a pseudo Gaussian distribution, then S will contain information about the location, extent and relative heights/depths of important image features such as peaks and troughs. The mask area and values contained in the mask are crucial in determining effective neighborhood of reconstruction. In effect,

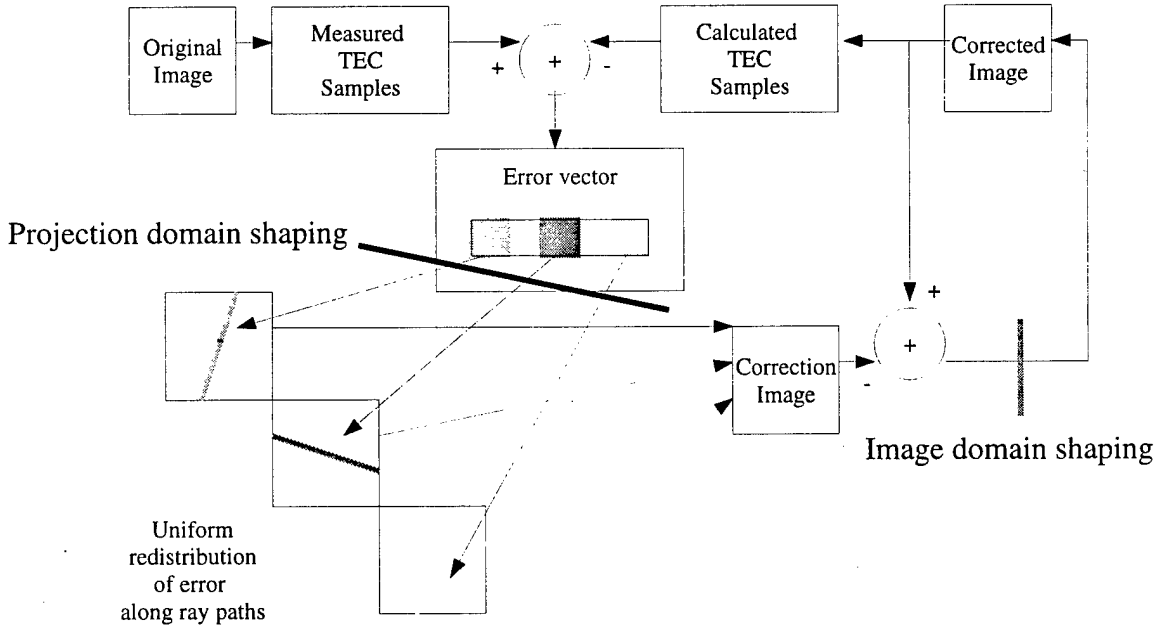

Figure 2. The standard Simultaneous Iterative Reconstruction Technique (SIRT) showing the two sites for volumetric correction in the VSIRT version.

it serves as a shape extracting and error based correction distributing template.

Comparison of the shape matrix of the updated reconstruction matrix with the shape matrices of a M priori images on a point to point basis, yields an error vector of length M for each point. The pixel values of the reconstruction contributing to this point of the shape matrix can then be updated based on the weighted error vector (the weights corresponding to inverse Euclidean distances) and distributed according to the mask values. Thus, with the Gaussian mask, the pixel directly beneath the mask center gets most of the correction and so on, causing the shape of the image is urged to conform to the optimal weighted shape for a given region by incurring minimal changes in actual values. The latter situation is due to the use of the inverse Euclidean distance weighting scheme. This procedure helps smooth out major discrepancies within a neighborhood that might arise because of independent profile distributions from different projection rays, while simultaneously avoiding the imposition of any global criteria for smoothness constraint.

In the actual implementation of the algorithm, the shape extraction and correction procedure was made effective after the 30th iteration, thus ensuring availability of substantial shape diversity in the reconstruction for meaningful interpretation of its shape matrix. Therefore, in each iteration of VSIRT, the net effect of volumetric correction is to shape and move fundamental features such as peaks, troughs and saddle points of the reconstruction towards the corresponding ones suggested by the composite shape formed by weighted a priori in the neighborhood of correction. The localized nature of the correction allows substantial flexibility in conforming to various regions of various a priori images. The weighting procedure ensures minimal disturbance i.e. conformity towards the shape that is naturally closer to the uncorrected reconstruction.

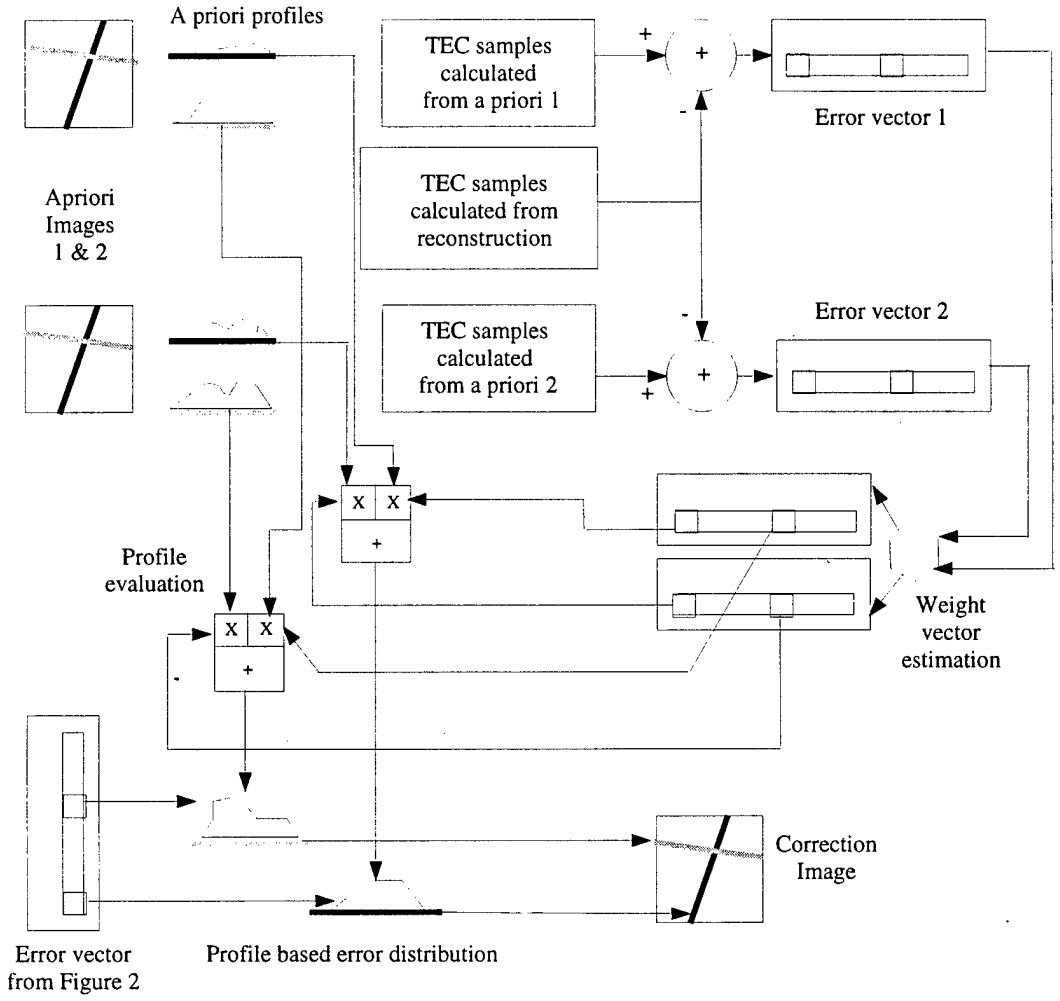

Figure 3. Projection domain correction in Volumetric SIRT

The extent of shape correction versus that achieved in the projection domain can be controlled externally by introducing a trade off parameter and also by regulating a multiplicative parameter for the former. Note that shape correction values occur in the range [-1,1], hence a multiplicative factor is required to make shape correction significant in to affect electron densities in the range 1e9-1e12/m^2 in the 2D plane of interest.

The overall success of this algorithm is not crucially dependent on initial guess of the image because of both types of volumetric corrections.

Results

All images used in the simulation were derived from the IRI-90 model. The TEC "readings" were collected in 64 projection sets of 6 samples each. Preliminary tests were carried out assuming equally spaced ground stations in a coplanar satellite-orbit receiver chain geometry. The test image was the ionospheric distribution at 0000 UT (1800 LT) over the 80W longitude, between the equator and the 30th parallel of the northern hemisphere. This image was simulated for June 21st, the summer solstice, during a year of quiet solar activity (SSN=10). All images are from ground level to 1000 km in the altitudinal direction.

The benefits derived from volumetric corrections in the projection error distribution phase of the algorithm can be assessed by considering the reconstructions shown in Figures 5(a) and (b). The former shows the reconstruction in 5 and its contour plot contrasted against the contour of the test image. Both show the lack of information in the vertical direction in contrast to the corresponding figures of 5(b) for the reconstruction with a priori guidance provided in the projection domain alone. With the exception of

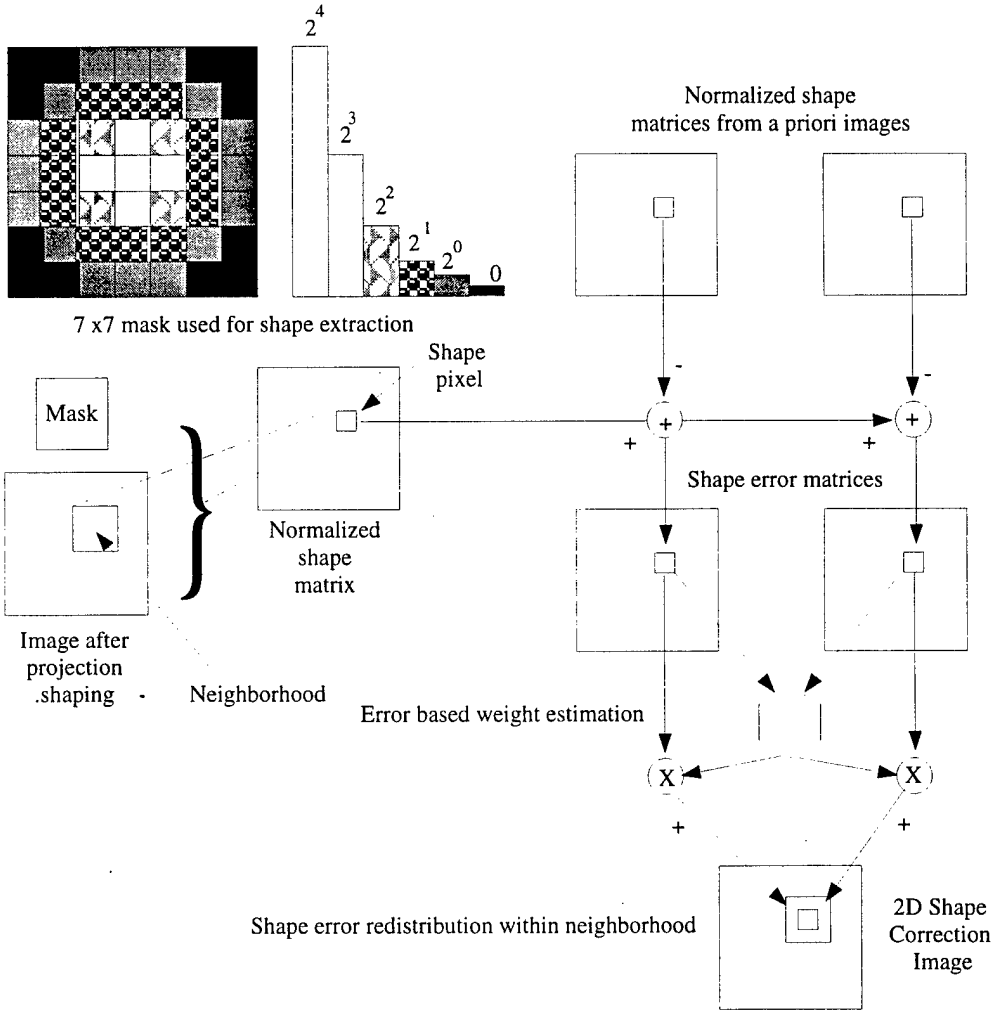

Figure 4. 2D Image domain shape correction in VSIRT

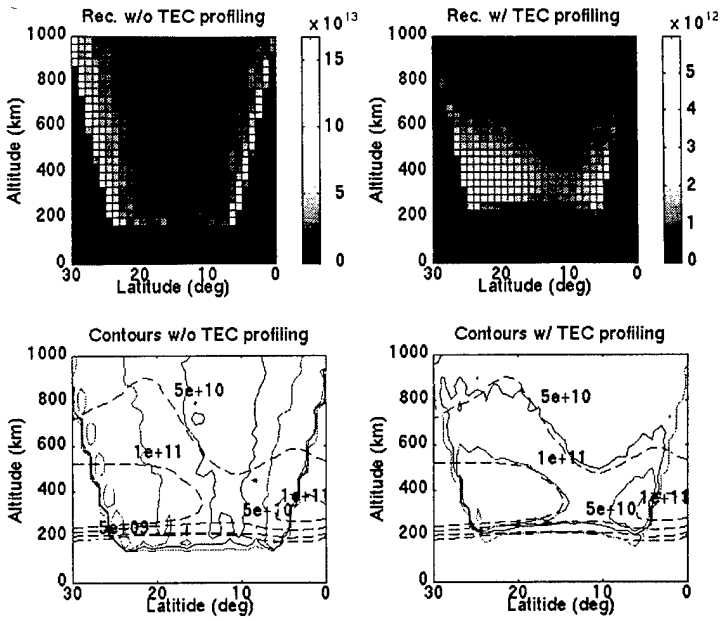

Figure 5. Improvement in reconstruction due to projection domain volumetric correction

pixels near the lateral edges of the view field, most contours of reconstruction run close to those of the test image.

Figures 6(a)-(d) show four suites of a priori images. Set 1A shown in Figure 6(a) is composed of ionospheric images within plus/minus two positions of the test image. 6(b) images are between three and four hours on either side. Set 1C shown in Figure 6(c) contains images of the ionosphere over the 24 hr period during the winter. Figure 6(d) corresponding to set 1D is for a day of high solar activity (SSN=110) during the Fall Equinox. Thus, the first set is most similar to the test image, the fourth, least.

Results of using projection domain distributions alone can be analyzed based on Figure 7. As expected, the reconstructions from a priori sets 1A and 1B are significantly better than those for the other two. Set 1A reconstructs the lower altitude ionospheric contours more accurately than any others. However, considering the variation in a priori images of the other sets from the test image, as shown in the Figures 6(a)-(d), it can been seen that positions of the northern half of the equatorial fountain above 21'N and 10' N trough have been faily well reproduced in sets 1B and C. The tip of the southern enhancement is not as accurately reconstructed probably due to its position at the extreme edge of the view area.

These reconstructions however, gain significantly in quality by the addition of image domain based volumetric correction. In many applications such as ROTHR (Relocatable Over The Horizon Radar), the location and electron density of principal features such as peaks and troughs are of greater importance than the rest of the image. Hence, it was deemed appropriate to analyze the nature of reconstruction achieved along certain crucial vertical and horizontal profiles. One such profile was chosen to be through the northern peak in the vertical direction at latitude 21.7241 degrees , another through the trough located above 9.3103 degrees north. One horizontal section through both peaks was considered at an altitude of 344.8 km above the earth's surface to compare the nature of reconstruction in the information rich horizontal direction versus that in the vertical direction.

Figures 8(a), 9(a) and 10(a) show the a priori profiles contrasted against the test image profiles for the north peak, the mid-trough and the horizontal two peak sections respectively. Figures 8(b), 9(b) and 10(b) show the reconstructions obtained using the four a priori suites for these profiles respectively. The profiles for greater quantities of image domain volumetric correction show greater conformity with that of the test image.

In Figure 8(b), reconstructions with sets 1A and B actually show movement of the peak altitude towards the ideal. Note also, the conformity of the upper and lower altitude profiles in each case. Set 1C profiles using winter time a priori for summer

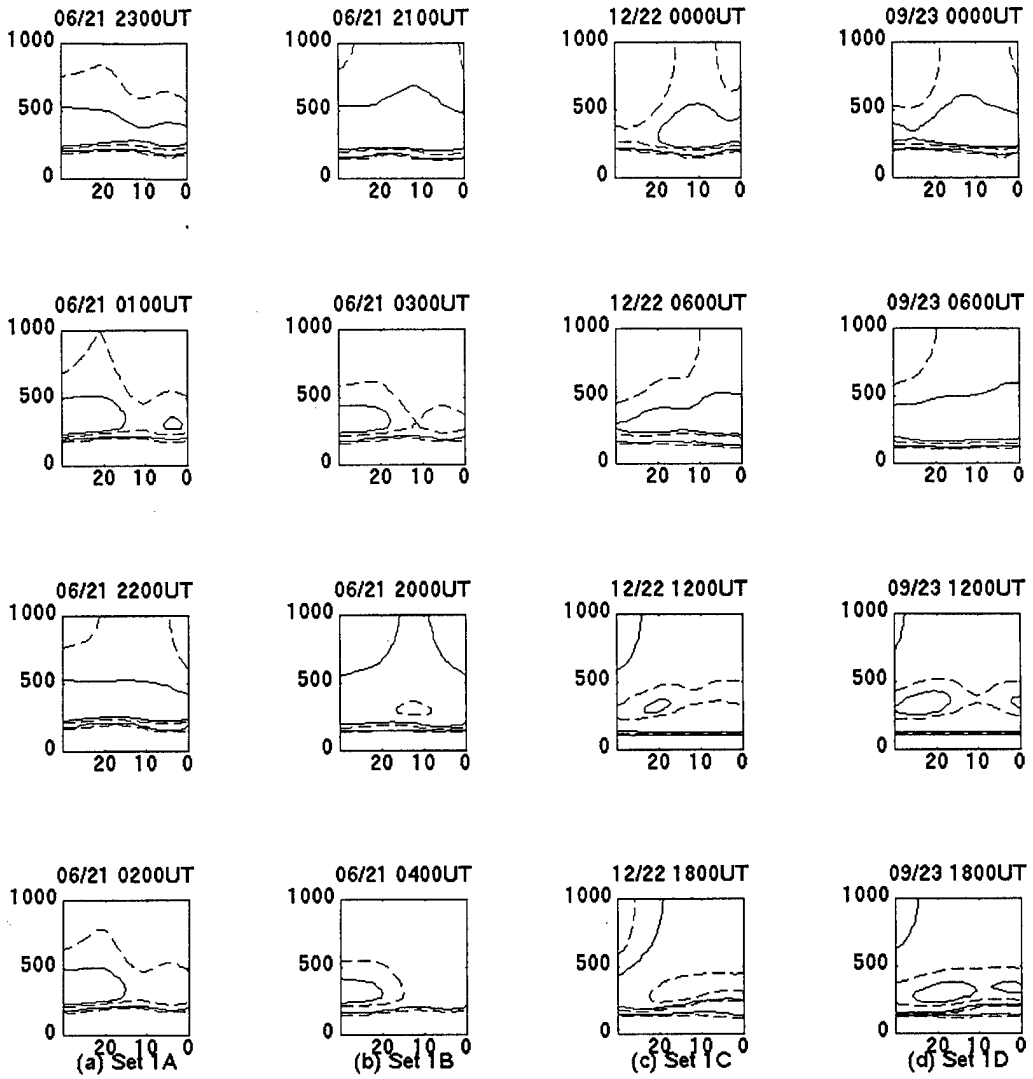

Figure 6. Four sets of a priori images for same region of ionosphere used in VSIRT reconstructions

time reconstruction shows a significant reduction in the 70%-30% profile of the northern peak although peak altitude is found to drift towards the ideal. This is because of the de-emphasis of the northern peak during the winter solstice. Reconstruction profiles using set D are steeper because the a priori are images for high solar activity. The sets C and D have been presented here to serve as examples of algorithm robustness to extremely dissimilar a priori. Comparing the profiles in Figures 8(a) and (b) for these sets provides proof of the above.

Considering the midtrough profiles in Figures 9(c) and (d), it is evident that whereas Sets 1A and B provide reasonable reconstructions, the convergence of the set 1C profile at a higher electron content regardless of quantity of image domain correction is owing to the higher electron concentrations of electron density in equatorward compared to that in the northern cross-section in winter. In peak and trough altitudes in Figures 8(b) and 9(b) were found to deviate from the ideal by at most 69 km, with an average of 22 km. Considering that each pixel accounts for 34.82 m in the altitudinal direction, judgement of the algorithm performance is best left to the reader and the application at hand. It is expected that finer resolution will provide better reconstruction fidelity.

Improvements achieved in the vertical direction are more apparent in the profiles in 10(a) and (b) of horizontal reconstruction. Granted that more information is available in the original measured data, and that image domain shape correction provided equal emphasis on all directions because a circular mask was chosen, proximity of horizontal profiles to the ideal when compared to those of the vertical ones

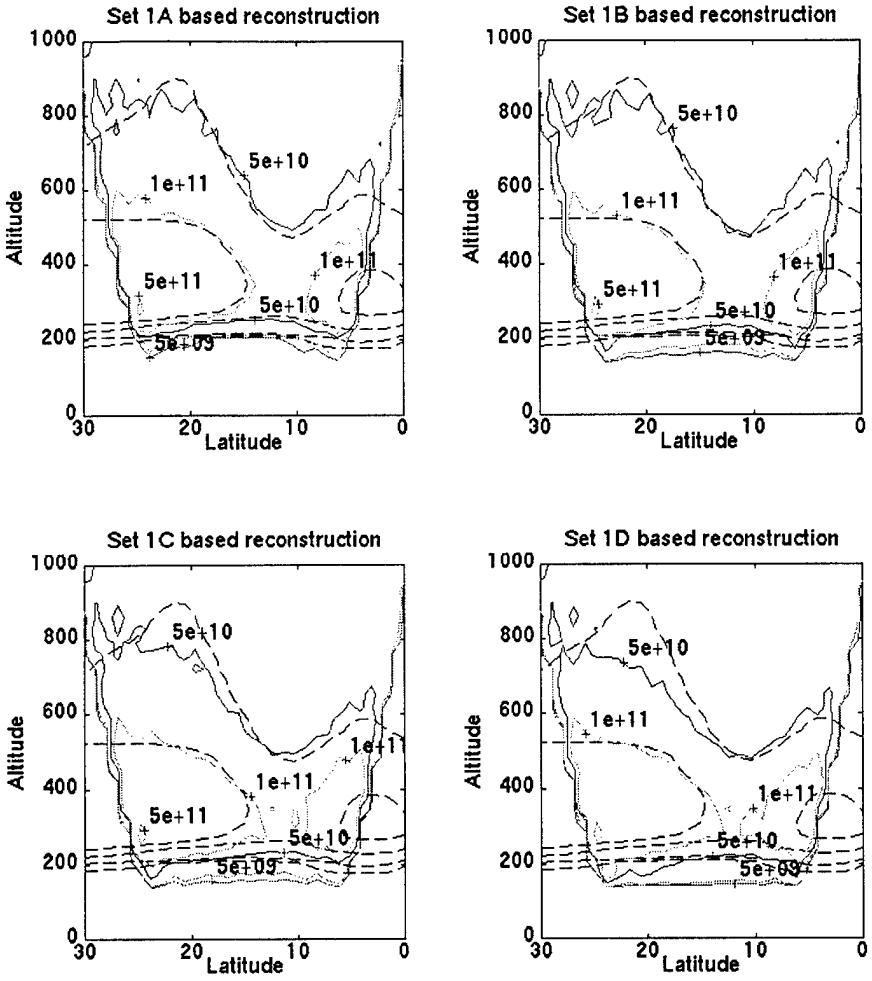

Figure 7. Reconstructions using 100% projection domain shaping

demonstrate the effectiveness of volumetric reconstruction. It must be mentioned that the reconstruction process was entirely free of any smoothing or averaging operation, hence, the serrated nature of the reconstructed horizontal profile.

The benefit of using image domain volumetric correction can also be viewed as an aid to systems with very few ground station receivers. Figures 11(a) and (c) correspond to set 1A based reconstruction for a 6 ground station chain whereas 11(b) and (d) are the result of a 4 receiver chain geometry. Compared to the top row which consists of pure projection domain correction, the reconstructions in the bottom row show greater smoothness of contours and conformity with test values. For both types of chains, the 70% reconstructions show greater peak height accuracy for the southern peak which is otherwise grossly overestimated in the 100% projection correction based reconstructions.

The above idea can be better understood by considering the composite profile maps of Figure 12. The first plot corresponds to set 1A based reconstructions of the northern peak whereas the second consists of sections through the trough. As is expected, profiles for 70%-30% tradeoff versus those from pure projection based correction are better representations of test peak height and profile. Although the four station reconstructions show two layers i.e. a double peak in both cases, the effect of 30% image domain based shape correction shows a smoothing trend towards the formation of a single peak at the true altitude. The trough profiles show better reconstruction , primarily because the region is well visible to both types of receiver chains because of its central location within the view area. Observe the progressive lowering of the saddle point peak towards the ideal density due to image domain correction both for the six and four station arrangements.

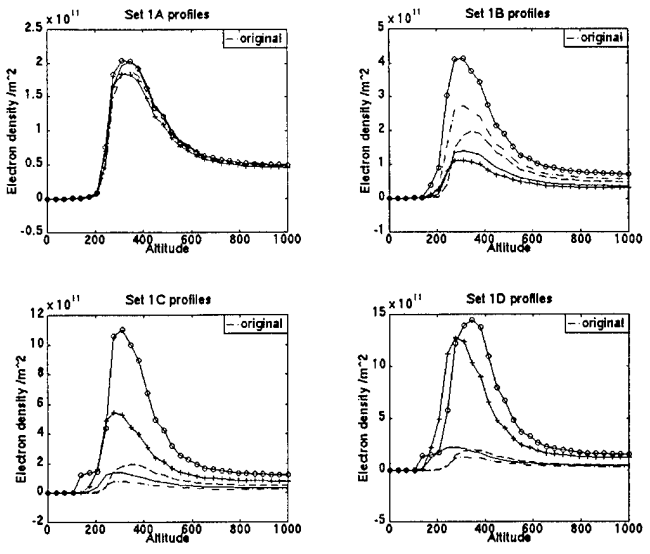

(a)

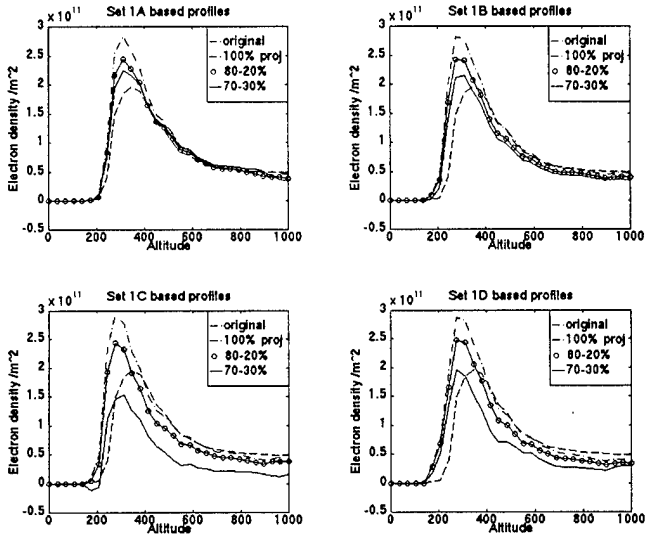

(b)

Figure 8. A priori and reconstruction profiles for the vertical section through the northern peak

Conclusion

Although the Volumetric SIRT algorithm has been used to reconstruct only IRI-90 based model images thus far, the extent of inter and intra a priori suite diversity cannot be underestimated. Whereas performing volumetric corrections in the projection domain alone leads to significant improvement in reconstruction, the role played by image domain volumetric correction is distinctly evident in Figure 8(b) for sets 1A and B where increased proportion of the latter actually moves the peak position to its ideal altitude. As with most reconstruction algorithms which use a priori image information, the final output of this algorithm does depend on the choice of a priori images.

The principal advantage of the VSIRT algoritm lies in the possibility of controlling the nature and extent of shape information at several points along each iteration. This allows significantly more opportunity for the reconstruction to find its natural shape with the aid of multiple a priori images than would be the case with fixed weights or corrections in any one domain. In brief the projection domain correction is to ensure maximal agreement with observed TEC measurements by redistribution error in the most likely profile along each ray. Subsequent two-dimensional shape correction serves to redistribute electron den-

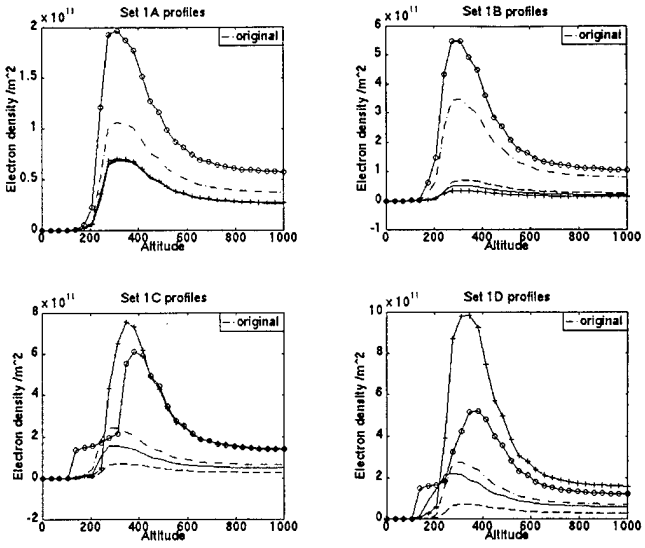

(a)

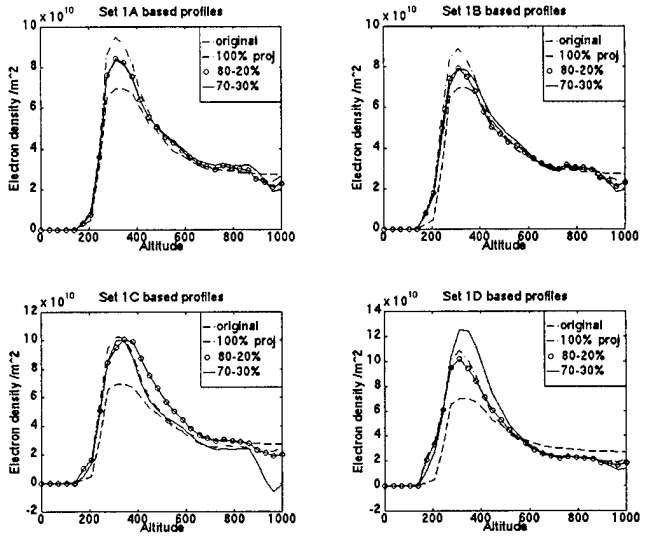

(b)

Figure 9. A priori and reconstruction profiles for the vertical section through the equatorial trough

sity values between pixels within each neighborhood to avoid local discrepancies that could arise because of dissimilar ray path profiles lying in close proximity.

The VSIRT algorithm allows substantial amount of localized access during the reconstruction process. Various points of control in the form of error based weight evaluation for individual ray path distributions and two-dimensional image neighborhoods as well as control over the tradeoff between projection and image domain shape corrections are present in the system. In addition, the size and the shape of the mask can be suited for preferential detection of the presence of certain shapes in the ionospheric plane of interest. Thus, the aim of detecting the natural shape of the reconstructed image is adequately fulfilled by the VSIRT algorithm using error based adjustments of ray path profiles in the projection domain and two dimensional shaping in the image domain.

Acknowledgements This work is supported by the grant NSF ATM 9696259 from the National Science Foundation and the grant ONR N00014–95–10850 from the Office of Naval Research, Washington DC, USA.

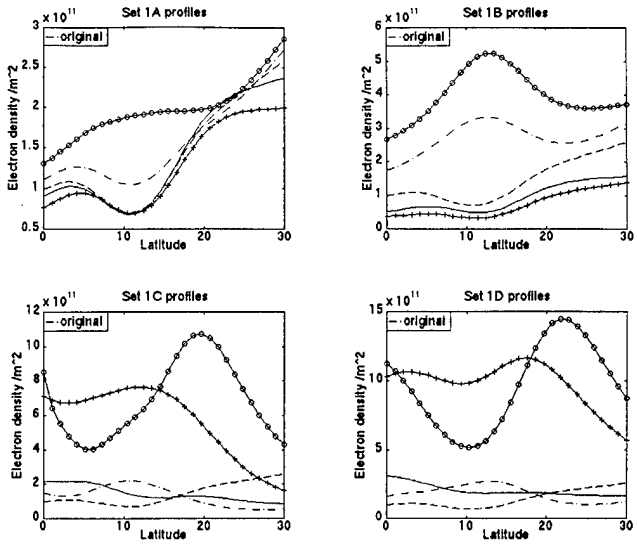

(a)

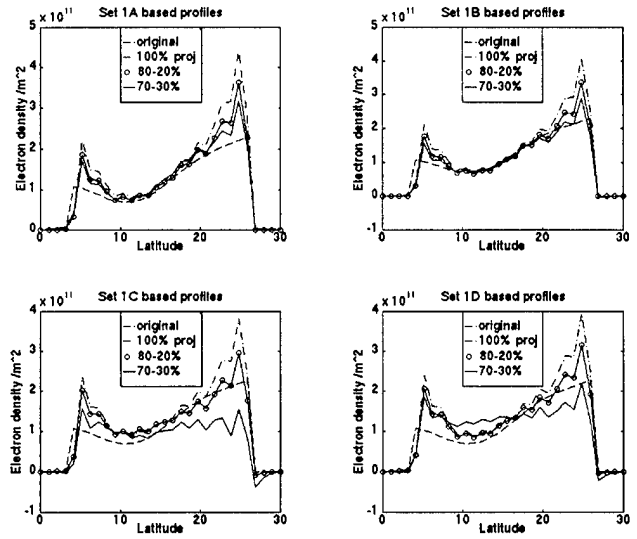

(b)

Figure 10. A priori and reconstruction profiles for the horizontal section through at 345 km altitude

References

1. Austen, J. R., S. J. Franke, and C. H. Liu, Ionospheric imaging using computerized tomography, *Radio Science*, 23(3), 299–307, 1988.
2. Davies, K., *Ionospheric Radio*, P. Peregrinus Ltd., London 1990
3. Raymund, T. D., Ionospheric tomography algorithms, *Int'l. J. Imag. Systems & Technol.*, 5(2), 75–85, 1994.
4. Raymund, T. D., S. J. Franke, and K. C. Yeh, Ionospheric tomography: its limitations and reconstruction methods, *J. Atmos. & Terr. Physics*, 56(5), 637–757, 1994.
5. Sutton, E. and H. Na, Ionospheric tomography using the residual correction method, *Radio Science*, 31(3), 489–496, 1996.
6. Yeh, K. C. and T. D. Raymund, Limitations of ionospheric imaging by tomography, *Radio Science*, 26(6), 1361–1380, 1991.

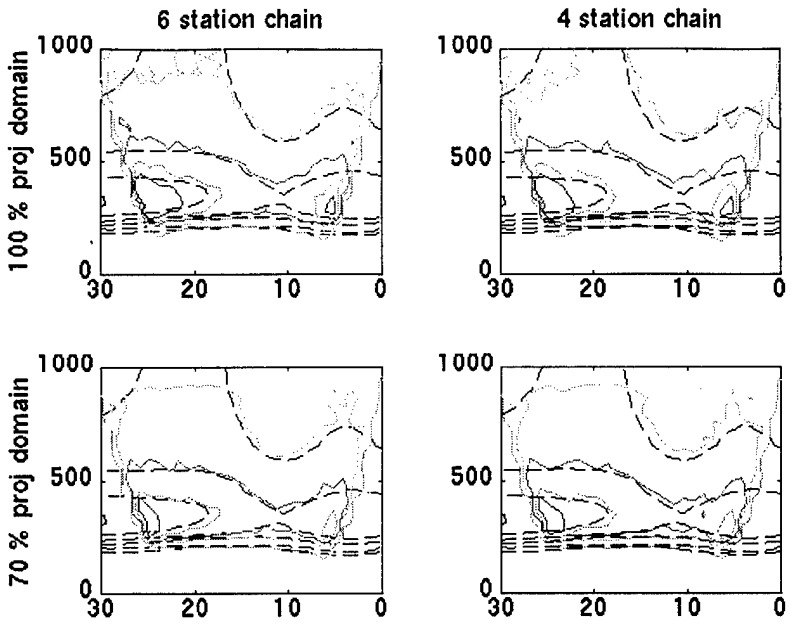

Figure 11. Reconstructions for two different system geometries. (a) 6 stations, 100% projection domain shaping. (b) 4 stations, 100% projection domain shaping (c) 6 stations, 30% image domain shaping (d) 4 stations, 30% image domain shaping

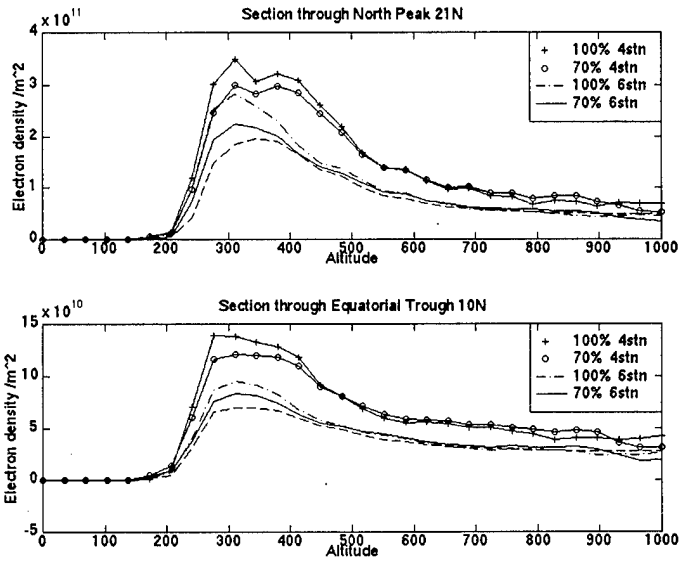

Figure 12. Reconstructed profiles for various imaging systems and extents of image domain shaping.